Enclosure 3

Westinghouse Responses to RAIs 2, 3, 4, 5, 6, 7, 8, 12, 13, and 14 on WCAP-18482-P/WCAP-18482-NP

(Non-Proprietary)

(25 Pages)

March 2021

Westinghouse Electric Company
1000 Westinghouse Drive
Cranberry Township, PA 16066

SFNB RAI 2

[

]^{b,c} This report shows that there is *dark zone* in the **ADOPT** fuel pellet and it is not centered in the pellet. Further, the TR states that the dark zone appearance is an effect of the large number of small pores. Grain boundaries cannot be detected inside the dark zone and grain size determination is not possible at various radii of the pellet. Also, the grain size was not possible to measure inside the dark zone, despite attempts with different etching times. Outside the dark zone the grain size is unchanged from the grain size as manufactured.

(a) Please provide details of the dark zone in **ADOPT** fuel pellet.

(b) What is the impact on the overall grain size measurement for **ADOPT** fuel due to the presence of the dark zone?

Response to SFNB RAI 2(a)

[

]^{b,c}

The 'dark zone,' which refers to the shaded concentric region of the pellet, originates after chemical etching in preparation for ceramography. Dark zones are the result of the etchant interacting with the intragranular pores and bubbles in the central region of the fuel, where higher temperatures are experienced. It is a common feature of UO_2 fuel irradiated to higher burnups and is not a property exclusive to the **ADOPT** pellet.

The etchant used interacts with grains differently depending on the crystal orientation. The H_2SO_4 acts as an acid and the H_2O_2 primarily as an oxidant, so some oxidation of the surface may also occur. Any inhomogeneities in the fuel will be attacked slightly preferentially. So, grain boundaries (GB) are preferentially attacked because of the edges and will appear dark because of the two crystal orientations (from each side of the GB) that are being etched creating a small ridge between the grains. Additionally, the freshness of the fuel sample will result in differences in the etching procedure, and also cause a slightly different result. Therefore, comparing the etching of two different samples is difficult.

The off-center dark zone, as depicted in Figure 1, indicates a power gradient across the fuel pin that is shifted, and it is an indicator that the moderation is stronger on that side of the fuel pin. Due to the etchant interacting with the intragranular pores and bubbles in the central region, grain boundaries cannot be distinguished in the dark zone, Figure 2.

[ ]b,c is presented in Figure 3 and Figure 4. Similar to the **ADOPT** rod, a dark zone is present, and the grain boundaries are difficult to distinguish due to the formation of the dark zone.

Response to SFNB RAI 2(b)

As discussed above, the grain size measurement was indeterminate due to the high amount of intragranular bubbles in this region. For comparison, ceramography of an alternative **ADOPT** rod, [ ]b,c is presented in Figure 5 and Figure 6. After etching, a dark zone is visible and individual grains are difficult to distinguish. The grain size measurements are presented in the Table 1.

b,c

b,c

b,c

[

]

b,c

b,c

b,c

b,c

SFNB RAI 3

Section 6.2.1.1.1 states: **[**

][a,c] Describe the impact on loss-of-coolant accident (LOCA) analysis due to the use of modified NFI model **[**

][a,c] Further justification is needed to provide clarification to the NRC staff.

Response to SFNB RAI 3

As described in Section 6.2.1.1.1 of WCAP-18482-P/WCAP-18482-NP, the pellet conductivity model used in the FULL SPECTRUM™ LOCA (FSLOCA™) evaluation model (EM) is used to determine the pellet conductivity at 95% theoretical density, and then the value is adjusted to account for densities other than 95%. Eq. 11-150 in WCAP-16996-P-A, Revision 1 shows the means by which the conductivity is adjusted for different theoretical density. It is effectively a linear scale factor which will result in a proportional change in adjusting from 95% to 97% or from 95% to **[ ]**[a,c].

As further discussed in Section 6.2.1.1.1 of WCAP-18482-P/WCAP-18482-NP, the primary importance of pellet conductivity for the LOCA response is related to the pellet temperatures during normal operation. For that purpose, the initial, steady-state pellet temperatures used in the FSLOCA EM simulations **[**

][a,c]

SFNB RAI 4

During the NRC regulatory audit for the Westinghouse TR WCAP-18482-P/WCAP-18482-NP, Revision 0, two (2) questions (topics) were asked regarding the distribution and re-distribution of the dopants in fresh fuel, as well as throughout irradiation. The intent of the following table is to resolve those questions, specifically those listed in the table below. Please provide the impact of distribution and re-distribution of dopants during irradiation on the behavior of **ADOPT** fuel during operation.

Topic Number	Subject	Response	Acceptable / Action Item	RAI Needed
4	Distribution of dopants in **ADOPT** fuel during irradiation	[ ]b,c		Combined with #6
6	Re-distribution of dopants during irradiation	[ ]b,c	Needs more	Yes

Response to SFNB RAI 4

Fresh fuel examination: The radial concentration of aluminum and chromium, in an unirradiated pellet, has been measured using wavelength dispersive spectrometry (WDS). The WDS examinations show a large statistical variation due to the low concentration of elements. [

]b,c More details are discussed in Section 3.1.3.1 of WCAP-18482-P/WCAP-18482-NP.

Steady-state, irradiated fuel examination: Electron probe microanalysis (EPMA) has been performed on two irradiated **ADOPT** rods to investigate the dopant migration behavior under steady state conditions.

- [

]b,c

- [

]b,c

[

]b,c

In addition to EPMA, laser ablation mass spectrometry was performed on the C1 **ADOPT** segment. This method offers an extremely high sensitivity to a wide range of elements. [

]b,c

Post-ramp, irradiated fuel examination: A section of the C1 **ADOPT** rod was ramp tested to a terminal power of 30 kW/m. Following ramp, laser ablation mass spectrometry, was performed on the segment. **[**

][b,c]

In summary, **[**

] [b,c]

b,c

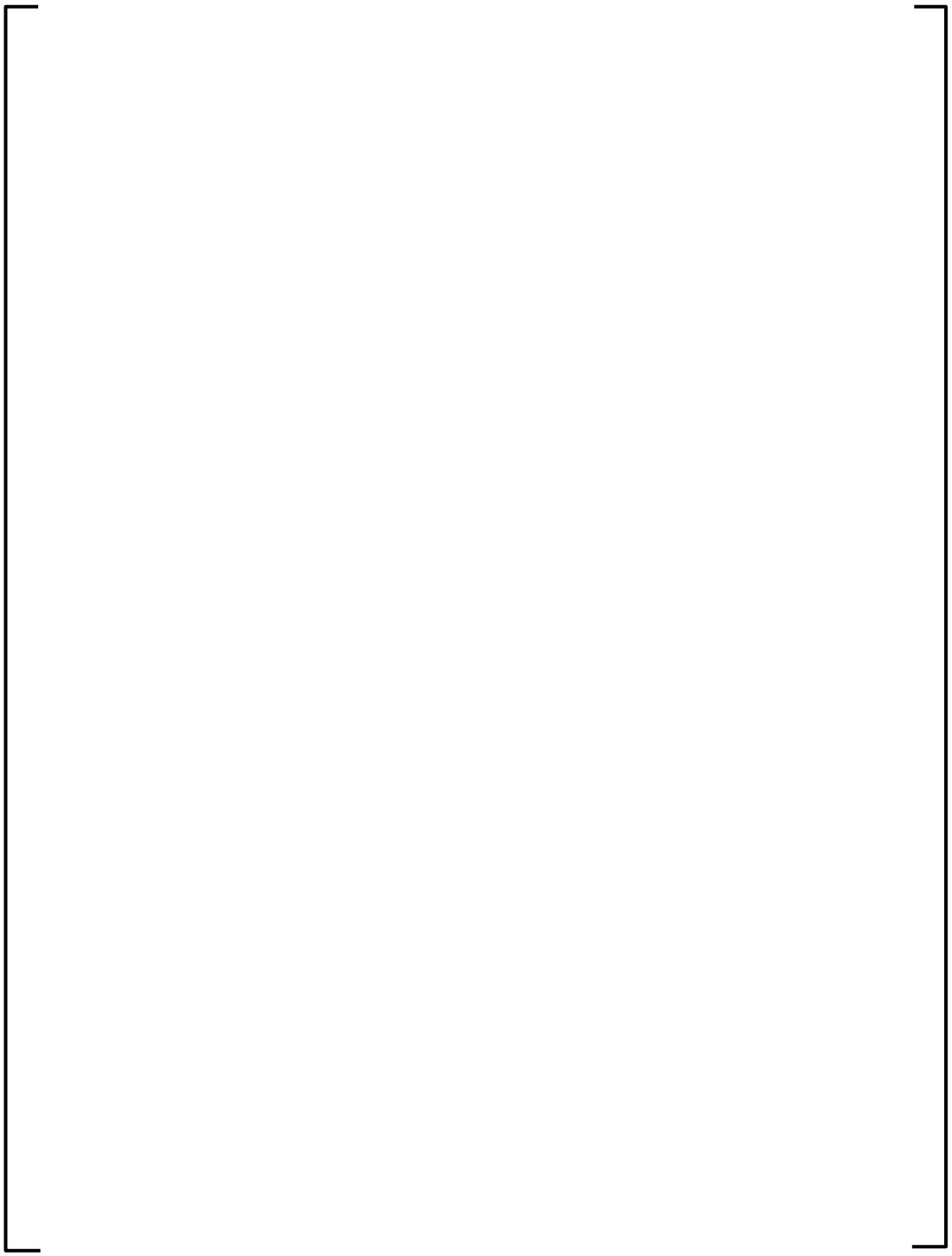

Figure 7: *SEM/EPMA of rod B5. Radial distribution of Al and Cr.*

b,c

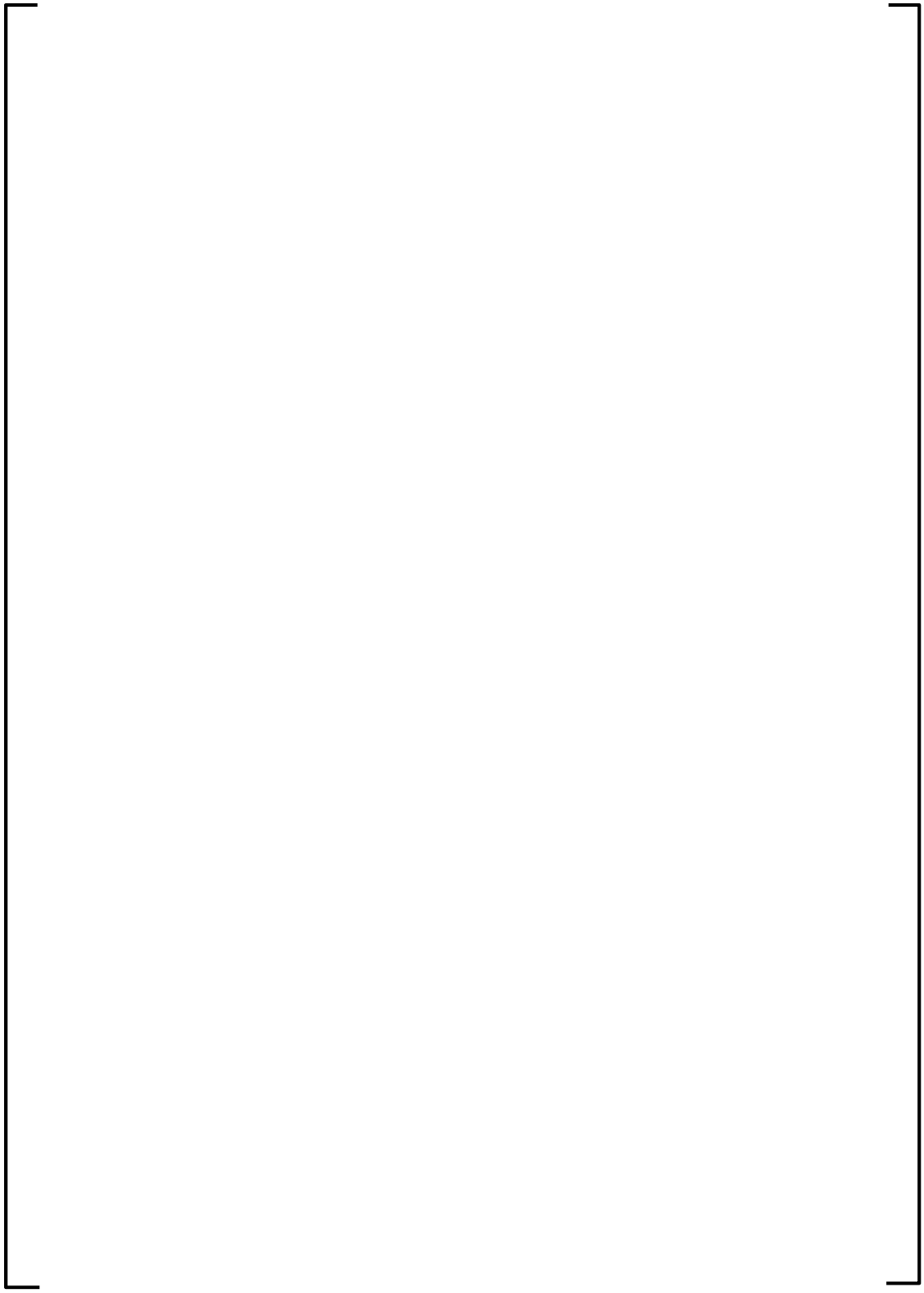

Figure 8: *SEM/EPMA of rod C1. Radial distribution of Al and Cr.*

Figure 9: *Radial profile using laser ablation for volatiles and additives in non-ramped* ***ADOPT*** *rod*

Figure 10: *Radial profile using laser ablation for volatiles and additives in ramped* ***ADOPT*** *rod*

SFNB RAI 5

Section 7.2.1.4.5 of PAD5 TR states: "Explicit calculation of the pellet radial power distribution (PD) is therefore only required for fuel designs not addressed within the range of the built-in pellet radial power distribution tables." What adjustment to PD is done to accommodate **ADOPT** fuel PD?"

Response to SFNB RAI 5

The PAD fuel pellet radial power distribution (RPD) model has been qualified for fuel enrichments between **[ ]**[a,c] The low concentration of chromium oxide (Cr_2O_3) and aluminum oxide (Al_2O_3) doping materials have minimal impact on the core reactivity due to the small absorption cross section. Additionally, the increase in theoretical density (TD) of **ADOPT** fuel **[ ]**[a,c] relative to standard uranium dioxide **[ ]**[a,c] will not have an appreciable impact on the RPD. The RPD models for UO_2 fuel therefore remain applicable to **ADOPT** fuel. If the **ADOPT** fuel stays within the predefined RPD limits for PAD **[ ]**[a,c] then no adjustments are required.

SFNB RAI 6

Based on item number 6 in the audit plan, the NRC staff requests Westinghouse to provide documentation with details of data analysis for irradiation programs described in Section 4; specifically ramp and bump testing, fission gas measurements, fuel pellet cracking, and cladding metallography. Chapter 5 of WCAP-18482-P/WCAP-18482-NP, Revision 0, characterizes the material properties and performance of ADOPT fuel pellets. Please confirm that the empirical data presented in this chapter was collected on fuel with the same specifications as the final production **ADOPT** fuel. Identify and disposition any differences, if they exist.

The following table shows the NRC staff concerns regarding Chapter 5 material properties and performance of **ADOPT** fuel during the audit. Please provide clarifications to the NRC staff concerns.

b,c

[

]

Response to SFNB RAI 6

Irradiation Programs Analysis Documentation:

Westinghouse has docketed two documents detailing the fission gas release analysis of **ADOPT** fuel operated **[**

][b,c]

Characterization and details of data analysis of **ADOPT** ramp testing will be provided as part of RAI 11 in a subsequent submittal.

ADOPT Fuel Specification Data:

In the following two figures, the manufacturing inspection data for production runs of **ADOPT** fuel since 2009 is presented. The dashed lines indicate the manufacturing specification requirements, which are also reflected in the fuel design constraints of the topical report:

[ ]b,c

For comparison, all manufacturing information of the data contained within the topical report is presented.

In Figure 11, a comparison of the density and grain size is presented; all experimental data presented in the topical report falls within the fuel design constraints requested for density and grain size.

In Figure 12, a comparison of the Al and Cr content is presented; all experimental data, with exception of the B2/R2 33004 segment, falls within the fuel design constraints requested for Al and Cr content. The B2/R2 data is presented in the topical because it is similar in grain size, density, and total additive content to **ADOPT**; similar behavior is expected.

Note that the KTH and IFA-677 Cr and Al content are presented as-manufactured (prior to sintering). Aluminum and chromium content were not measured after sintering for these samples. **[**

]b,c

b,c

***Figure 11: ADOPT** Manufacturing Data, Density vs grain size*

b,c

***Figure 12: ADOPT** Manufacturing Data, Al v. Cr content*

SFNB RAI 7

Chapter 5.2.2 of WCAP-18482-P/WCAP-18482-NP, Revision 0, demonstrates that **ADOPT** fuel pellets promote larger fuel rod growth. In Figure 6-3, PWR fuel rod growth measurements are plotted against the PAD5 upper bound fuel rod growth model. As shown in Figure 6-3, the level of confidence in the upper bound growth model has clearly diminished based on the increased **ADOPT** fuel rods growth.

a. Please explain why the existing upper bound model remains valid.

b. If applicable, please describe the process for gathering future rod length measurements to confirm or revise the empirically based, high confidence growth model(s) used in fuel design analyses.

Response to SFNB RAI 7a.

Available measured data for **ADOPT** fuel demonstrates increased fuel rod growth relative to uranium dioxide (UO_2) fuel. This is evidenced by Figures 5-3, 5-4 and 5-5 of the **ADOPT** fuel topical report (WCAP-18482-P/WCAP-18482-NP). The increased growth is caused by the earlier pellet-cladding contact due to the increased density and reduced densification of **ADOPT** fuel. Earlier contact results in generally higher axial length growth. The effects of the **ADOPT** rod growth deviations at low and high fluence values are discussed below.

Low Fluence Axial Rod Growth

The axial growth for Pressurized Water Reactor (PWR) **ADOPT** fuel is clearly underpredicted at low fluence values. Lower growth at this time in life would cause an increase in rod internal pressure (RIP) due to the reduction in void volume (pressure and volume being inversely related). Higher RIP delays pellet-cladding gap closure, which is non-conservative for transient cladding strain and cladding fatigue. For transient cladding strain, which is limiting near the point of gap closure, the delayed contact means that the fuel has less potential energy during a limiting Condition II overpower transient. Lower Condition II transient powers cause less thermal expansion of the fuel during the accident. This is non-conservative for transient cladding strain. However, scoping studies have shown that rod growth uncertainties have a negligible impact on the strain criterion (**[ ]**[a,c] as defined in Section 7.3.2 of WCAP-17642-P-A, Rev. 1).

Earlier pellet-cladding contact also affects cladding fatigue because of the increased cyclic loading seen by the fuel cladding. Axial growth uncertainty has a greater impact on cladding fatigue than it does for transient cladding stress **[ ]**[a,c]**.** However, cladding fatigue is a non-limiting design criterion, and the increase in upper bound (UB) cumulative fatigue because of slightly higher RIP early in life is expected to be minor, especially as the growth uncertainty is statistically convoluted with other fatigue uncertainty cases. In other words, any slight increase in cumulative fatigue resulting from of an underprediction in axial rod growth is inconsequential in comparison to the available margin to the design limit.

High Fluence Axial Rod Growth

The measured growth data for **ADOPT** falls within the PAD5 UB growth model at high fluences, as shown in Figure 6-3 of the **ADOPT** fuel topical report (WCAP-18482-P/WCAP-18482-NP). As discussed in Section 5.9 of the PAD5 topical report (WCAP-17642-P-A, Rev. 1), measurements from two plants, designated as Plant L and Plant T, contain significantly higher rod growth data compared with all other samples. A conservative approach was taken for PAD5 by **[**

][a,c]. The result is a conservatively high UB growth model in PAD5 which remains bounding with respect to many of the **ADOPT** fuel measured data, including all data points at high fluence. However, the confidence level for axial growth at high fluence has diminished.

The primary fuel performance criteria affected by axial rod growth at high fluence (and burnup): RIP and fuel rod growth. Decreased axial growth is conservative for RIP because of the associated reduction in available void volume. RIP calculations are therefore performed with LB growth models, so the application of the UO_2 growth model for **ADOPT** fuel is conservative and acceptable.

The acceptance limit for fuel rod axial growth is that the fuel rods are designed with adequate clearance between the fuel rod and the top and bottom nozzles to accommodate the differences in the growth of fuel rods and the growth of the assembly without interference. A loss of confidence for the UB axial growth of **ADOPT** fuel would be non-conservative because it would lead to earlier contact between the fuel rods and the top and bottom nozzles. However, as with cladding fatigue, there is margin to the fuel rod growth design limit. The UB axial growth rate can be increased by **[** **]**[a,c], and all current Westinghouse fuel lattices with **ZIRLO** High Performance Fuel Cladding Material will continue to meet the design limit up to **[** **]**[a,c] burnup. For **Optimized ZIRLO** High Performance Fuel Cladding Material, which demonstrates reduced axial growth relative to **ZIRLO** cladding, the UB axial growth rate can be increased by **[** **]**[a,c] and still meet the design limit up to **[** **]**[a,c] burnup.

As additional measured data for **ADOPT** fuel is gathered (see response 'b' below), it may become preferential to re-evaluate the growth model for PAD5. In the interim, however, the current PAD5 growth model remains applicable for **ADOPT** fuel. The loss of confidence in the UB growth is either conservative (e.g., for RIP), negligible (e.g., for strain), or can be offset with available design margin (e.g., fatigue and fuel rod growth).

Response to SFNB RAI 7b.

Rod growth measurements will continue to be taken to confirm or revise the current empirically based growth model. Post-irradiation exams (PIEs) are planned for current and future Lead Test Rod (LTR) and Lead Test Assembly (LTA) programs containing **ADOPT** fuel. This includes both the ongoing Byron Unit 2 Accident Tolerant Fuel (ATF) LTR program and future LTR and LTA programs. Growth measurements are obtained using the Fuel Rod Handling Tool (FRHT) motor resolver in conjunction with the High Definition Shielded Video (HDSV) camera and High Definition Fuel Inspection

Recording Station (HD FIRSt) video recording system to measure and record the individual length of each inspected rod.

All additional measured data for **ADOPT** fuel shall eventually be incorporated into the PAD5 growth model. As stated in the executive summary for WCAP-18482-P/WCAP-18482-NP, Westinghouse is not currently seeking to take full advantage of all the benefits of **ADOPT** fuel. Subsequent licensing submittals are planned to further expand the approval of **ADOPT** fuel and more fully exercise the benefits of the fuel material. The appropriateness for the use of "simplified" models with the current submittal is based on extensive operating experience with **ADOPT** fuel in Europe, as well as demonstration that the inclusion of fuel dopants to UO_2 fuel does not introduce any new failure modes or require new or revised specified acceptable fuel design limits (SAFDLs). Discussion on the continued applicability of the existing PAD5 growth model is included in response 'a' above.

Future submittals for **ADOPT** fuel shall explicitly incorporate the planned additional test data, including axial fuel rod growth measurements. It may be preferential to modify the existing PAD5 growth model based on this new data. The current growth model is a function of only fluence and cladding material. An improved model can be developed to explicitly account for the differences between UO_2 and **ADOPT** fuel and the role of pellet-cladding contact on axial growth. As shown in Figures 5-3, 5-4 and 5-5 of the **ADOPT** fuel topical report (WCAP-18482-P/WCAP-18482-NP), Boiling Water Reactor (BWR) rods close the gap later than PWR rods and show the growth difference at higher fluences. For both BWR and PWR rods, the differences between **ADOPT** and UO_2 fuel rods are about **[ ]**^{a,c} at high fluences. While the final form of the model depends on the new measured axial growth data garnered from current and future ATF LTR and LTA programs, it is conceivable that a delta growth can be added to the UO_2 rod growth to account for the difference in gap closure, a saturated growth difference **[ ]**^{a,c}, and the transition from gap closure to the saturated delta growth. The uncertainty of **ADOPT** fuel rod growth is expected to be smaller due to high density and inherently smaller uncertainty in densification. Regardless of the form these model changes may or may not take, it is incumbent on Westinghouse to ensure that it continues to utilize an empirically based, high confidence growth model to perform fuel design analyses both now and in the future.

SFNB RAI 8

Section 5.3 of WCAP-18482-P/WCAP-18482-NP, Revision 0, describes the empirical database used to confirm the adequacy of the fission gas release model for **ADOPT** fuel pellets. Most of these measurements were performed using poolside gamma scanning, a technique that has now been qualified and its accuracy confirmed by sending some of the measured rods to hot cells for rod puncturing. Please provide details of the qualification of the poolside gamma scanning technique and comparison to hot-cell data.

Response to SFNB RAI 8

Poolside measurements of fission gas release (FGR) are relative comparisons of Kr-85 in the plenum and Cs-137 in the pellet stack. Kr-85 is the only radioactive fission gas with a half-life long enough to be measured nondestructively. The amount of Kr-85 released to the free rod volume can be determined by gamma spectrometry measurements in the plenum of a fuel rod. By comparing the amount in the free rod volume with the total amount formed by fission, the released portion can be calculated. By assuming that release rates for all fission gases are similar, the total amount of released fission gases can be assessed.

The qualification and verification of the poolside gamma scanning technique has been performed by comparison with destructive testing performed in a hotcell of the same or symmetrical fuel rods. Table 2 presents a comparison of poolside data and hotcell destructive testing on **[ ]**[b,c] and the results agree well, with only a very minor deviation between poolside and hotcell measurements, see Figure 13.

Poolside FGR measurements taken from large campaigns are typically confirmed by destructive hotcell examination of a smaller number of rods. If necessary, the examination data is used to develop an adjustment factor. In this case, the data agrees well, and no adjustments of the poolside data is necessary.

Table 2: *Comparison of poolside FGR measurements and hotcell FGR measurements*

[ ]b,c

b,c

Figure 13: *Comparison of poolside FGR measurements and hotcell FGR measurements*

SFNB RAI 12.

With the expansion of load following in the U.S. nuclear fleet, PWRs may become increasingly susceptible to pellet-clad interaction (PCI)/SCC cladding damage during power maneuvering. While explicit NRC-approved fuel maneuvering limits and guidance are not mandated, licensees must have well defined power maneuvering guidance (e.g., ramp rate restrictions, pre-conditioning), based on irradiated fuel rod ramp testing, to ensure no fuel damage during normal operation. How has PCI/SCC been addressed for **ADOPT** fuel designs? Has power ramp testing been conducted to confirm existing power maneuvering guidance or establish new guidance?

Response to SFNB RAI 12

[

]^{b,c} Post ramp destructive PIE indicates that **ADOPT** fuel should provide more PCI/SCC margin than UO_2 fuel. The Westinghouse PWR maneuvering guidance is based on an extensive Zircaloy-4, **ZIRLO** and **Optimized ZIRLO** cladding ramp test database. The purpose of the limits is to allow for stress relaxation to limit the maximum cladding tensile stress from PCMI to levels below the threshold for PCI/SCC. The limits for the rate of power increase are designed to allow for stress relaxation due to cladding creep during continuous power increase.

With respect to **ADOPT**'s PCI resistance, it is expected that **ADOPT** fuel will exhibit improved PCI behavior. As discussed in Section 3.3.2 of WCAP-18482-P/WCAP-18482-NP, Revision 0, the high temperature creep rate is higher in **ADOPT** fuel than that of conventional UO_2; this enhanced viscoplastic behavior should provide a PCI benefit, as the pellet deforms under its own internal stresses and fills in as-manufactured dishes. Ceramography of ramped doped fuel similar in grain size and density, confirmed this behavior, as presented in Section 4.1.3 of the topical report. Additionally, incipient cracking of the liner was determined to be slightly improved.

[

]^{b,c,e}

SFNB RAI 13

Section 6.2.4 of WCAP-18482-P/WCAP-18482-NP, Revision 0, dispositions **ADOPT** fuel with respect to the applicability of existing guidance related to radionuclide release fractions, timing of releases, and elemental composition of releases. The potential impacts of the dopants and the larger grain size with respect to intergranular hold-up, rate of release of short-lived radionuclides, chemical interactions with dopants, fuel fragmentation, fuel melting temperature, etc. need to be addressed.

Response to SFNB RAI 13

A larger grain size results in lower fission product release rates from the fuel pellets according to Equation 5.7 of NUREG/CR-6261 ("A Summary of ORNL Fission Product Release Tests With Recommended Release Rates and Diffusion Coefficients," September 1995). Similarly, **[**

][a,c]. WCAP-18482-P/WCAP-18482-NP Section 3.2.3 concludes that there is no appreciable difference in the melting point of UO_2 and **ADOPT** fuel, so that would not result in earlier or higher release. **[**

][a,c]

The chemistry of fission products released from the fuel in a severe accident is not affected by the addition of the dopants. Obviously, noble gas fission products are nonreactive and are unaffected by anything. The chemistry of the iodine released from the fuel is dominated by the formation of CsI salt. Cesium is a fission product that is in abundance with respect to iodine and cesium is released from the fuel at a rate similar to iodine (both are volatile), and therefore iodine and cesium releases are not affected by the addition of Al_2O_3 and Cr_2O_3. The formation of other fission product compounds is affected primarily by the distribution of oxygen between the elements in the fuel pellet. There is already plenty of oxygen in the system in the UO_2 and PuO_2, as well as in the water, so the addition of oxygen from the dopants is negligible. As shown on the Ellingham diagram, at temperatures near the melting temperature, the oxygen potential is dominated by U and Pu with respect to the dopants Cr and Al. Therefore, the addition of the dopants does not significantly change the chemistry of the fission products released from the pellets during a core melt accident.

SFNB RAI 14

Please submit on the docket to the NRC Document Control Desk the following documents for further information to enable accurate safety evaluation:

1. **[**

   ][b,c]

2. **[**

   ][b,c]

3. **[**

   ][b,c]

4. JNST- 2006, "Advanced Doped UO2 Pellets in LWR Applications," Jakob ARBORELIUS, Karin BACKMAN, et.al Journal of Nuclear Science and Technology

5. [

]b,c

Response to SFNB RAI 14

With this transmittal, requested documents 1,2,3, and 5 are being submitted to the NRC Document Control Desk. Document 4 is publicly available.